remote sensing

MDPI

Article

Influences of Seasonal Soil Moisture and Temperature on Vegetation Phenology in the Qilian Mountains

Xia Cui [1,*], Gang Xu [2], Xiaofei He [2] and Danqi Luo [2]

[1] Key Laboratory of Western China's Environmental Systems (Ministry of Education), College of Earth and Environmental Sciences, Lanzhou University, Lanzhou 730000, China
[2] State Key Laboratory of Grassland Agro-Ecosystems, College of Pastoral Agriculture Science and Technology, Lanzhou University, Lanzhou 730020, China; xugang@lzu.edu.cn (G.X.); hexf21@lzu.edu.cn (X.H.); luodq20@lzu.edu.cn (D.L.)
* Correspondence: xiacui@lzu.edu.cn

Abstract: Vegetation phenology is a commonly used indicator of ecosystem responses to climate change and plays a vital role in ecosystem carbon and hydrological cycles. Previous studies have mostly focused on the response of vegetation phenology to temperature and precipitation. Soil moisture plays an important role in maintaining vegetation growth. However, our understanding of the influences of soil moisture dynamics on vegetation phenology is sparse. In this study, using a time series of the normalized difference vegetation index (NDVI) from the moderate resolution imaging spectroradiometer (MODIS) dataset (2001–2020), the start of the growing season (SOS), the end of the growing season (EOS), and the length of the growing season (LOS) in the Qilian Mountains (QLMs) were extracted. The spatiotemporal patterns of vegetation phenology (SOS, EOS, and LOS) were explored. The partial coefficient correlations between the SOS, EOS, and seasonal climatic factors (temperature, precipitation, and soil moisture) were analyzed. The results showed that the variation trends of vegetation phenology were not significant ($p > 0.05$) from 2001 to 2020, the SOS was advanced by 0.510 d/year, the EOS was delayed by 0.066 d/year, and the LOS was prolonged by 0.580 d/year. The EOS was significantly advanced and the LOS significantly shortened with increasing altitude. The seasonal temperature, precipitation, and soil moisture had spatiotemporal heterogeneous effects on the vegetation phenology. Overall, compared with temperature and soil moisture, precipitation had a weaker influence on the vegetation phenology in the QLMs. For different elevation zones, the temperature and soil moisture influenced the vegetation phenology in most areas of the QLMs, and spring temperature was the key driving factor influencing SOS; the autumn soil moisture and autumn temperature made the largest contributions to the variations in EOS at lower (<3500 m a.s.l.) and higher elevations (>3500 m a.s.l.), respectively. For different vegetation types, the spring temperature was the main factor influencing the SOS for broadleaf forests, needleleaf forests, shrublands, and meadows because of the relative lower soil moisture stress. The autumn soil moisture was the main factor influencing EOS for deserts because of the strong soil moisture stress. Our results demonstrate that the soil moisture strongly influences vegetation phenology, especially at lower elevations and water-limited areas. This study provides a scientific basis for better understanding the response of vegetation phenology to climate change in arid mountainous areas and suggests that the variation in soil moisture should be considered in future studies on the influence of climate warming and environmental effects on the phenology of water-limited areas.

Keywords: vegetation phenology; Qilian Mountains; soil moisture; remote sensing

Citation: Cui, X.; Xu, G.; He, X.; Luo, D. Influences of Seasonal Soil Moisture and Temperature on Vegetation Phenology in the Qilian Mountains. *Remote Sens.* **2022**, *14*, 3645. https://doi.org/10.3390/rs14153645

Academic Editor: Zhuosen Wang

Received: 2 June 2022
Accepted: 26 July 2022
Published: 29 July 2022

1. Introduction

Vegetation plays an important role in ecosystem carbon and hydrological cycles [1,2] and is a sensitive indicator of ecosystem response to climate change. Vegetation phenology, which is the periodic life activity of plants, provides an independent measure of how

ecosystems respond to climate change [3] and varies significantly according to climate zone and vegetation type, especially in temperate and northern regions [4,5]. Affected by climate change and human activity, the start of the growing season (SOS), the end of the growing season (EOS), and the length of the growing season (LOS) show substantial interannual variability [6]. Phenological changes result in small-area changes in plant activity within the community and large-area changes in overall land surface processes, such as the carbon budget, surface energy flux, and regional climate [7]. Therefore, understanding phenological variation and its response to climate change is critical for improving terrestrial biosphere models and climate models [8].

Current research methodologies on vegetation phenology mainly include the traditional ground observation method and satellite remote sensing monitoring method. Traditional ground observations can provide detailed specific plant phenology information at the species-scale or individual plant scale but have limitations in terms of observational stations and spatial coverage [9]. In addition, most ground observation sites only focus on cultivated plants rather than natural vegetation [10]. Remote sensing data from satellites can provide long time series and a high temporal resolution vegetation index (VI) and have been widely applied in large-scale vegetation phenology monitoring [11]. The satellite remote sensing monitoring method primarily uses time series VIs, and the normalized difference vegetation index (NDVI) is the most commonly used VI [12]. The NDVI is simple to calculate and sensitive to plant growth and can track seasonal dynamic changes in vegetation [13].

Climate changes can be directly reflected in vegetation phenology [6]. Temperature can be considered the most important factor affecting vegetation phenology in many regions. Numerous studies have found that advances in spring phenology at middle and high latitudes are primarily controlled by increased global surface mean temperature [14–17]. Additionally, precipitation is a key factor in regulating vegetation phenology, particularly in water-limited arid and semiarid regions [18]. For example, Ren et al. [19] showed that the influence of precipitation on the interannual variation in the SOS and EOS is more important than that of temperature in the Inner Mongolian Autonomous Region. Compared with precipitation, soil moisture is the most direct water supply for vegetation and is susceptible to drought, which can affect vegetation phenology [20]. Some observational studies have suggested that soil water availability is also an important factor that can trigger vegetation growth in water-limited areas [21,22]. An understanding of the impact of soil moisture dynamics on vegetation phenology is very important and can increase our understanding of the influence of climate change on ecosystems. However, there are insufficient studies related to this topic.

The Qilian Mountains (QLMs) are located in the arid/semiarid region of northwestern China, which is a transitional zone between the Qinghai–Tibet Plateau (QTP), Loess Plateau, and Inner Mongolia Plateau. The QLMs have a vulnerable ecosystem and complex climate, and the hydrothermal conditions differ from east to west [23]. In recent years, the QLMs have experienced significant climate changes, which involve a significant trend of warming and wetting, frequent climate anomalies [24], and local vegetation becoming sensitive to climate changes [25]. In addition, the large east–west span and spatial heterogeneity among the vegetation types in the QLMs lead to enormous differences in the response relationship between the vegetation phenology of different vegetation types and climatic factors. Soil moisture plays an essential role in maintaining vegetation growth, especially in arid and semi-arid regions [20]. Soil moisture in the QLMs increases with an increase in altitude and is heterogeneous between different types of land cover [26]. Due to the complex topography and climatic conditions, the ecosystems in the QLMs are fragile and sensitive to climate change, and thus it is necessary to systematically explore the effects of temperature, precipitation, and soil moisture on vegetation phenology.

Based on moderate resolution imaging spectroradiometer (MODIS) NDVI time series products from 2001 to 2020, this study extracted the SOS, EOS, and LOS for the QLMs' vegetation and analyzed the characteristics of the changes in vegetation phenology and

the response relationship between vegetation phenology and driving factors, including temperature, precipitation, and soil moisture. The main objectives of this study were to (1) investigate the characteristics of the spatiotemporal patterns of vegetation phenology in the QLMs during the period 2001–2020, (2) evaluate the effects of seasonal temperature, precipitation, and soil moisture on the SOS and the EOS in the study area, and (3) explore the relationship between the phenology of different elevation zones, vegetation type, and climatic factors in the QLMs. This study can contribute to our understanding of the mechanism of the effects of climate change on vegetation phenology in arid mountain areas, and the findings enable the prediction of the future evolution of ecosystems and the implementation of effective ecosystem management.

2. Data and Methods

2.1. Study Area

The QLMs represent the largest mountain system in the marginal northeast of the QTP, which crosses Gansu Province and Qinghai Province. The geographical coordinates lie between 93°25′–103°50′E and 35°52′–39°52′N, with a total area of approximately 184,000 km^2. The terrain gradually rises from northeast to southwest, and the average elevation exceeds 3500 m (Figure 1). The northern slope of the QLMs contain the headwaters of three inland rivers (Heihe, Shulehe, and Shiyanghe rivers) in China [27]. Qinghai Lake is the largest inland saltwater lake in China and is fed from the south slope of the QLMs. The QLMs belong to the midlatitude northern temperate zone, which has a typical continental plateau climate [28]. Due to the obvious vertical zonality and horizontal zonality, the water and heat conditions in the Qilian Mountains dramatically vary spatially. Precipitation mainly occurs in the summer and decreases from east to west, increasing with altitude, but temperature shows the reverse pattern [25]. The main vegetation types in the region include broadleaf forests, needleleaf forests, shrublands, meadows, grasslands, and deserts, and the natural ecosystems are fragile and sensitive to climate change because of complex topographic and climatic conditions.

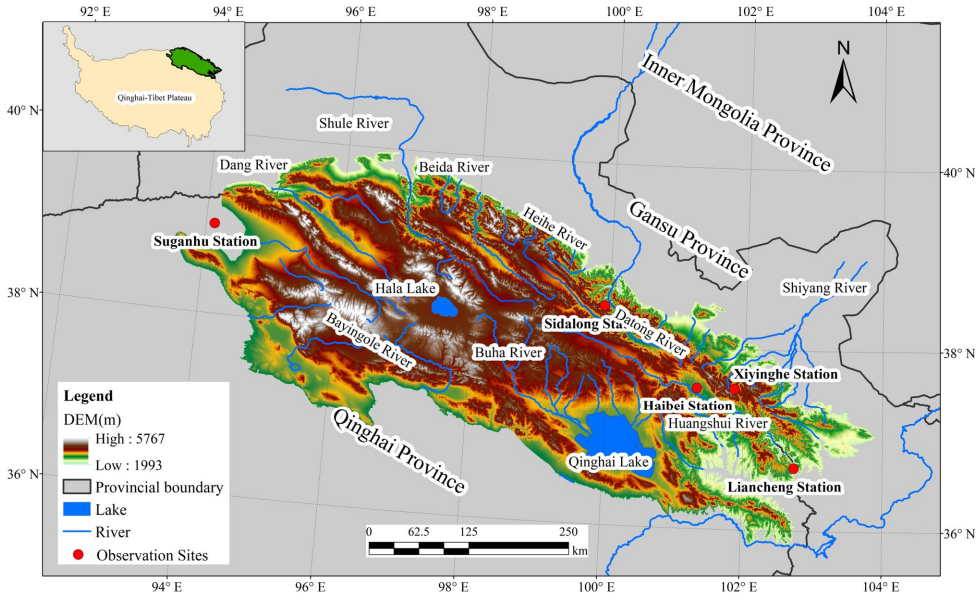

Figure 1. Geographical location of the Qilian Mountains.

2.2. Data Sources

NDVI time series have been widely used as an important proxy for quantifying vegetation photosynthetic activity. The MODIS NDVI products (MOD13A2) from 2001 to 2020 with a 1 km spatial resolution and 16-day time step were used in this study. The NDVI data were obtained from NASA (https://lpdaac.usgs.gov, accessed on 20 November 2021) and were preprocessed using the MODIS reprojection tool (MRT) for band extraction and

mosaic, format, and projection conversion. We removed pixels with average annual NDVI values (2001–2020) < 0.1 to prevent the interference of nonvegetation signals [18,29].

The ground-based phenology data were collected from the vegetation phenological observation datasets at Haibei station from 2006 to 2015, which were provided by the Chinese Ecosystem Research Network (CERN) (http://www.cnern.org.cn, accessed on 17 December 2021). In addition, the phenology data of Sidalong station, Liancheng station, Xiyinghe station, and Suganhu station from 2020 were obtained from the National Tibetan Plateau Data Center (https://data.tpdc.ac.cn/en/, accessed on 17 December 2021).

Monthly temperature and precipitation data from 2001 to 2020 were obtained from the National Tibetan Plateau Data Center (http://data.tpdc.ac.cn, accessed on 22 April 2021). These datasets were spatially downscaled from CRU TS v4.02 with WorldClim datasets based on the delta downscaling method and were evaluated using the data of 496 national weather stations across China. The evaluation indicated that the downscaled dataset is reliable for investigations related to climate change across China [30]. The monthly surface soil moisture data (0–7 cm) from 2001 to 2020 were obtained from ERA5-Land and used to represent the water availability indicator to evaluate the water content impacts on vegetation phenology. ERA5-Land provides a soil moisture reanalysis dataset of $0.1^\circ \times 0.1^\circ$ from 1950 to the present. The monthly soil moisture data from ERA5-Land were resampled to the same resolution as the vegetation phenology data using a bilinear interpolation algorithm. The digital elevation model at a spatial resolution of 1 km was obtained from the Resource and Environmental Science and Data Center (http://www.rsdc.cn/, accessed on 17 December 2021).

2.3. Methods

2.3.1. Extraction of Vegetation Phenology

The NDVI time series involves some noise caused by clouds or poor atmospheric conditions and needs to be smoothed using a filter. In this study, NDVI was smoothed using a seven-parameter double logistic function proposed by Gonsamo et al. [31] to reconstruct the NDVI time series at a daily temporal resolution:

$$f(x) = \alpha_1 + \frac{\alpha_2}{1 + e^{-\partial_1(x-\beta_1)}} - \frac{\alpha_3}{1 + e^{-\partial_2(x-\beta_2)}} \quad (1)$$

where f(x) is the fitted NDVI at day x; x is a specific day of year (DOY); α_1, α_2, α_3, ∂_1, ∂_2, β_1, β_2 are smoothing parameters; α_1 is the background NDVI value; α_2 is the early summer plateau; α_3 is the amplitude of the late summer plateau; ∂_1 and ∂_2 represent the transitions in the slope coefficient; and β_1 and β_2 are the midpoints at the start and end of the growing season transitions, respectively.

For the fitted *NDVI* time series, the dynamic threshold derived from each pixel was used to determine the SOS and EOS. In this method, the SOS and EOS are defined as the DOY when the $NDVI_{ratio}$ reaches a certain threshold during the *NDVI* rising stage in spring and decline stage in autumn. The $NDVI_{ratio}$ is calculated as:

$$NDVI_{ratio} = \frac{NDVI_x - NDVI_{min}}{NDVI_{max} - NDVI_{min}} \quad (2)$$

where $NDVI_x$ represents the *NDVI* value on day x and $NDVI_{max}$ and $NDVI_{min}$ are the maximum and minimum *NDVI* values in the annual NDVI time series, respectively. In this study, the dynamic threshold was defined as $NDVI_{ratio}$ values of 30% and 50% to determine the SOS and EOS, respectively. The LOS was the difference between the SOS and EOS.

2.3.2. Trend Analysis

The temporal trends in the time series of the vegetation phenology were calculated by the Theil–Sen median slope estimator [32] at the pixel level. The Theil–Sen median slope estimator is a nonparametric median-based slope estimator that is less susceptible to noise and outliers [33]. A positive Theil–Sen slope indicates a delayed or extended trend,

while a negative value indicates an advanced or shortened trend. The Mann–Kendall (MK) method [34] was used to determine the significance of the long-term advanced/delayed trend in vegetation phenology. In our study, the significance level was based on the MK test value, and $p < 0.05$ was defined as statistically significant. The combined use of the Theil–Sen median slope and MK trend test classified vegetation phenological parameters into five categories, namely, "significant advanced/shortened", "insignificant advanced/shortened", "no change", "insignificant delayed/extended", and "significant delayed/extended".

2.3.3. Partial Correlation Analysis

Partial correlation coefficients were calculated to examine the correlation between vegetation phenology and seasonal driving factors (temperature, precipitation, and soil moisture). In our analysis, the seasons were defined as spring (March–May), summer (June–August), and autumn (September–November). The second-order partial correlation coefficient was calculated as follows:

$$r_{12,34} = \frac{r_{12,3} - r_{14,3} \times r_{24,3}}{\sqrt{(1 - r_{14,3}^2) \times (1 - r_{24,3}^2)}} \quad (3)$$

where $r_{12,34}$ represents the partial correlation coefficient of variables 1 and 2 after controlling for variables 3 and 4. $r_{12,3}$ represents the first order partial correlation coefficient and was computed as follows:

$$r_{12,3} = \frac{r_{12} - r_{13} \times r_{23}}{\sqrt{(1 - r_{13}^2) \times (1 - r_{23}^2)}} \quad (4)$$

where r_{12}, r_{13}, r_{23} represent the Pearson's correlation coefficients between variables 1 and 2, 1 and 3, and 2 and 3, respectively. After we calculated the partial correlation coefficient values, Student's t-test was used to identify the significance of the coefficient, and only the pixels with a significance level of $p < 0.05$ were considered significant. To determine the influence of terrain and vegetation types on the linkage between vegetation phenology and seasonal driving factors, the partial correlation coefficients in different elevation zones and different vegetation types were also analyzed in our study. The elevation was reclassified into four classes (1: <3000 m a.s.l., 2: 3000–3500 m a.s.l., 3: 3500–4000 m a.s.l., and 4: >4000 m a.s.l.).

3. Results

3.1. Temporal and Spatial Variation in Vegetation Phenology

The vegetation phenology derived from the satellite data was consistent with ground observations at the Xiying River, Liancheng, Suganhu, and Sidalong stations in 2020 and the Haibei station from 2006 to 2015. The correlation coefficient (R^2) between the SOS and field data was 0.536 ($p < 0.01$), the mean absolute error (MAE) was 9 d, the root mean square error (RMSE) was 11 d, the R^2 was 0.533 ($p < 0.01$), the MAE was 5 d, and the RMSE was 6 d between the EOS and field data (Figure S1). Based on the validation results described above, the remote sensing monitoring method adopted in this paper can accurately reflect vegetation phenological characteristics in the QLMs.

The interannual changes in vegetation phenology in the QLMs from 2001 to 2020 showed different fluctuation ranges (Figure 2). There was an advanced SOS trend of 0.510 d/year and an extended LOS trend of 0.580 d/year. There was a delayed EOS trend at a rate of 0.066 d/year, which is only a slight change. However, no significant changes were found in these vegetation phenology parameters ($p > 0.05$).

The vegetation phenology parameters varied with altitude (Figure 3). With an increase in altitude, the SOS showed a gentle upward trend, but the correlation between the SOS and altitude was weak ($p > 0.05$). Conversely, with an increase in altitude, the EOS gradually advanced and the LOS gradually shortened. There was a significant negative correlation between the altitude and both EOS and LOS ($p < 0.05$), and the correlation coefficients were high ($R^2 \geq 0.899$). The SOS tended to be delayed by 0.20 d/100 m, while the EOS

tended to advance by 0.60 d/100 m, and the LOS tended to extend by 0.80 d/100 m with increasing altitude.

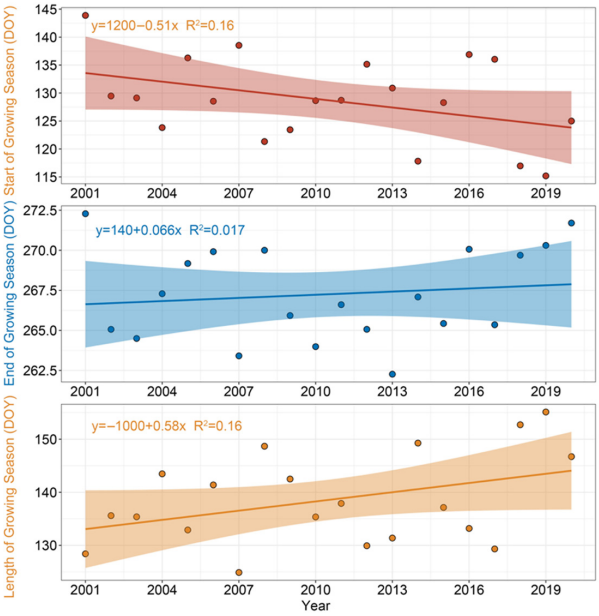

Figure 2. Interannual changes in vegetation phenology in the QLMs.

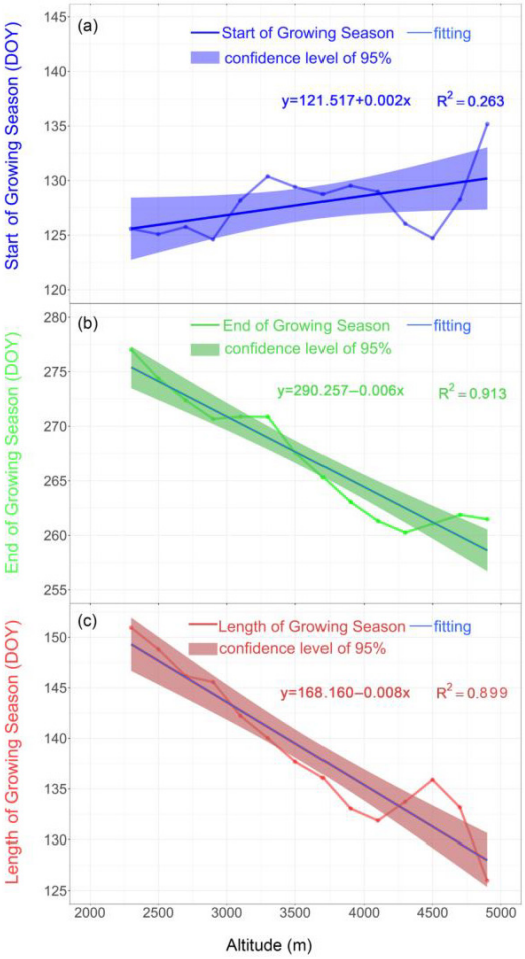

Figure 3. Characteristics of the changes in the SOS (**a**), EOS (**b**), and LOS (**c**) with altitude.

The multiyear average spatial distribution of phenology in QLMs from 2001 to 2020 is shown in Figure 4a,c,e. From east to west, the vegetation phenology showed evident changes. Overall, the SOS in the study area mainly occurred from 115 days to 150 days, which accounted for more than 80% of the vegetation region. The earlier SOS was mainly seen in the eastern and western QLMs, and the later SOS was mainly distributed in the central section. In addition, the multiyear mean EOS of vegetation phenology varied between 255 and 275 d (more than 80% of the overall pixels) from the middle of September to early October. The EOS showed the opposite pattern in terms of spatial distribution compared with the SOS; it was earlier in the central section of the QLMs and later in the western and eastern sections of the QLMs. Due to the combined effects of SOS and EOS, the LOS was mainly between 110 and 160 d. The spatial pattern of LOS was similar to that of EOS, whereby the LOS was shorter in the central section of the QLMs and longer the eastern and western sections of the QLMs.

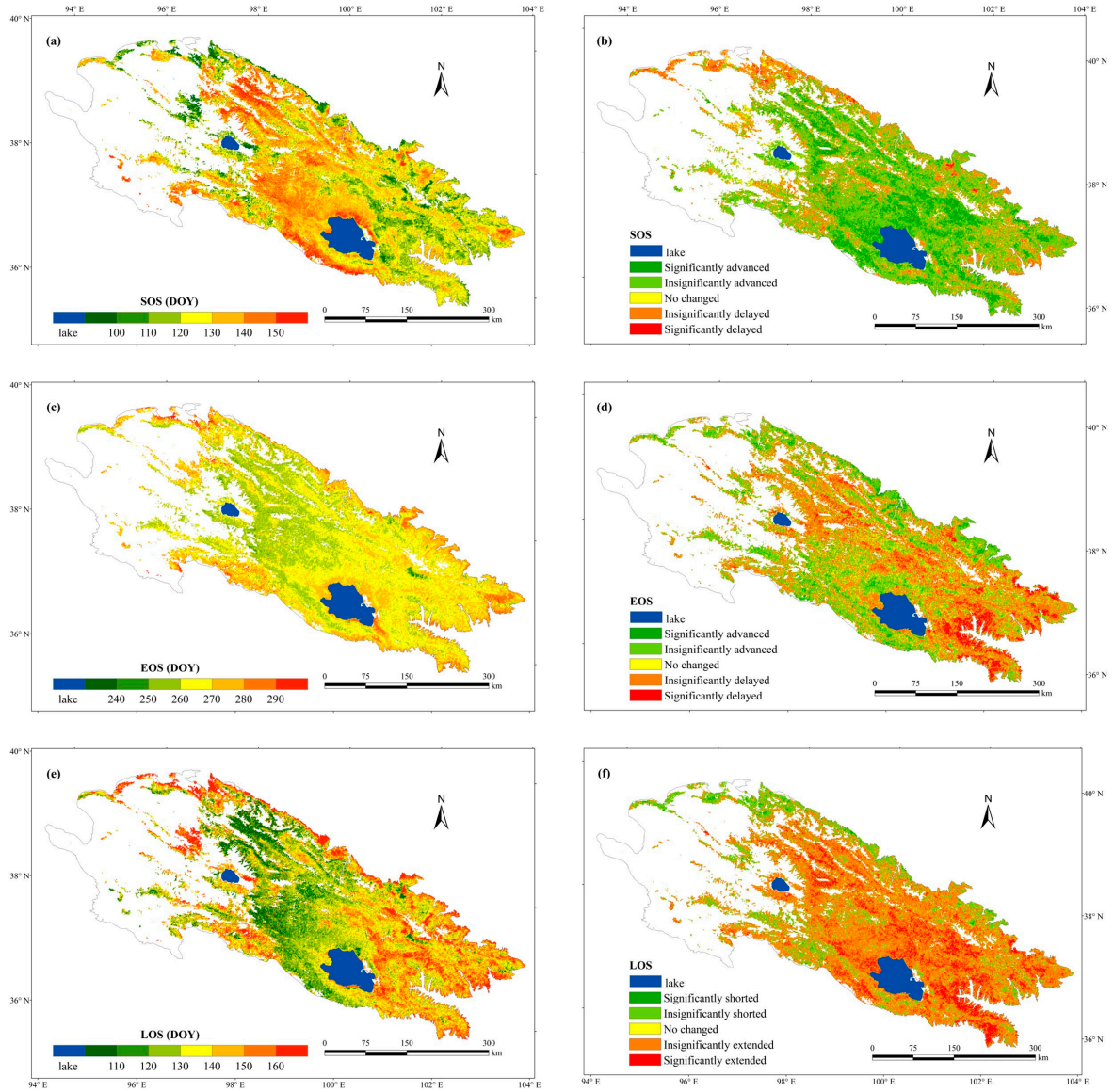

Figure 4. Spatial distribution and the change trend of vegetation phenology parameters. The left side represents the spatial pattern of the average value of the SOS (**a**), EOS (**c**), and LOS (**e**) from 2001 to 2020. The right side represents the spatial distribution of the change trend of the SOS (**b**), EOS (**d**), and LOS (**f**) from 2001 to 2020. The trends are considered significant for pixels according to the MK test ($p < 0.05$).

Figure 4b,d,f and Table 1 show the spatial distribution of the vegetation phenology trend in the QLMs from 2001 to 2020. A total of 72.37% of the vegetation pixels showed an advancing trend of SOS from 2001 to 2020. A total of 13.85% of pixels, which were mainly concentrated in the central and eastern sections of the QLMs, showed a significant advancing trend of SOS. A few areas in the northwest of the QLMs showed a delayed trend of SOS, whereas only 1.44% of the total land area was significantly delayed. Regions with delayed EOS accounted for 47.59% of the vegetation pixels in the study area from 2001 to 2020 and were mainly located in the eastern and central sections of the QLMs. In addition, the areas with advanced EOS were mainly located on the northern margins and at the northwest of Qinghai Lake. Approximately 6.8% of vegetation pixels had a significant delayed trend in terms of the EOS, and 3.9% of vegetation pixels had a significantly advanced trend. There was an overall extended LOS trend for most parts of the vegetation area (71.66% of the vegetation pixels) from 2001 to 2020, with 12.65% being significantly extended and only 1.87% being significantly shortened. The areas with extended LOS trends were mainly distributed in the central and eastern sections of QLMs.

Table 1. The percentage of different trends of vegetation parameters based on MK analysis across the QLMs.

Vegetation Phenology	Insignificantly Advanced/Shortened	Insignificantly Delayed/Prolonged	Significantly Advanced/Shortened	Significantly Delayed/Prolonged
SOS	58.52%	19.62%	13.85%	1.44%
EOS	36.57%	40.79%	3.90%	6.80%
LOS	23.42%	59.01%	1.87%	12.65%

3.2. Response of Vegetation Phenology to Seasonal Driving Factors

The spatial distribution of the partial correlation coefficients between seasonal driving factors and vegetation phenology metrics are displayed in Figure 5. For the QLMs, the SOS was negatively correlated with spring temperature in 73.81% of vegetation pixels, while 21.21% of pixels showed a significant correlation ($p < 0.05$) and were mainly located in the eastern and central parts of the study area (Figure 5a). The percentage of negative and positive correlations between the SOS and spring precipitation was similar (Figure 5c), with a significant negative correlation occurring in the northeast of Hala Lake. More than half of the vegetation pixels (61.34%) of the SOS had a negative correlation with spring soil moisture, of which 9.18% of pixels showed a significant negative correlation (Figure 5e), mainly at the west of Qinghai Lake. The results above indicate that the increases in spring temperature and soil moisture likely cause the SOS to advance in most part of the QLMs.

The partial correlation coefficients between the EOS and autumn temperature showed that the EOS was positively correlated with temperature in 65.20% of vegetation pixels, and 9.89% of the areas passed the significance test (Figure 5b). Approximately 56.19% of the vegetation pixels showed a negative correlation between the EOS and autumn precipitation, and only 4.75% of the areas passed the significance test (Figure 5d). For autumn soil moisture, positive correlations between the EOS and soil moisture occurred in 60.44% of the total vegetation pixels, and approximately 9.50% of the pixels showed a significant positive correlation ($p < 0.05$, Figure 5f), most of which were distributed west of Qinghai Lake and southeast of Hala Lake. In total, the autumn temperature and soil moisture influenced the EOS in most areas, and the increase in autumn temperature and soil moisture likely caused the EOS to be delayed.

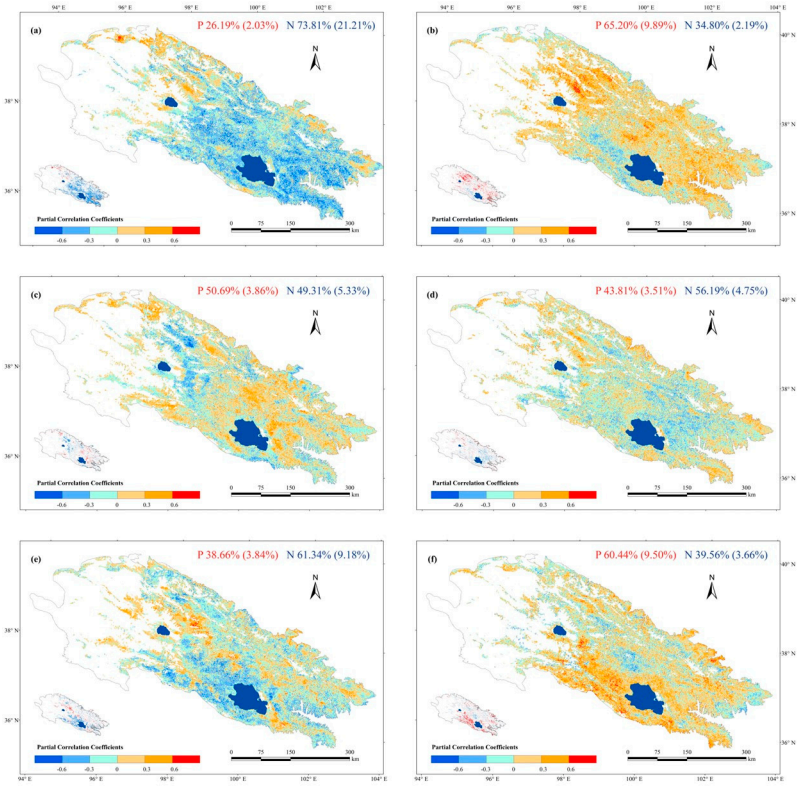

Figure 5. The partial correlation coefficients between vegetation phenology parameters and seasonal driving factors. (**a**,**c**,**e**) represent the partial correlation coefficients between the SOS and spring temperature, precipitation, and soil moisture, respectively. (**b**,**d**,**f**) represent the partial correlation coefficients between the EOS and autumn temperature, precipitation, and soil moisture, respec-tively. The inset panels on the bottom left of each subpicture present pixels with a significantly ($p < 0.05$) negative (blue) and positive (red) correlation. The percentages of positive (P) and negative (N) correlations (the values in brackets indicate the percentage of significant correlations) are shown at the top of each subpicture.

3.3. Vegetation Phenology Parameters Response to Seasonal Driving Factors Based on Different Elevation Zones

The driving factors had different effects on vegetation phenology depending on elevation. The results of the partial correlation analysis between the vegetation phenology parameters (SOS, EOS) and seasonal driving factors (temperature, precipitation and soil moisture) for different elevation zones are shown in Figure 6. A mainly negative correlation occurred between the SOS and spring temperature (the percentage of significant negative correlation ranged from 14.59% to 24.87%) at different elevation zones. At middle elevations (3000–4000 m a.s.l.), more than 76% of the vegetation pixels showed a negative correlation between the SOS and spring temperature (Figure 6a), and more than 24% of the areas passed the significance test. The SOS was mainly negatively correlated with spring soil moisture (more than 61%) at the <4000 m elevation zone, and the percentage of areas that passed the significance test at the 95% level ranged from 7.24% to 12.5% (Figure 6c). However, the SOS had the opposite correlation with spring soil moisture in the highest elevation zone (mainly positive), 7.63% of the areas showed a significant positive correlation (Figure 6c). Compared with spring temperature and soil moisture, spring precipitation had a weaker influence on the SOS at the four elevation zones, and the areas of positive and negative correlation between spring precipitation and the SOS were similar, with few pixels showing a significant correlation (Figure 6b).

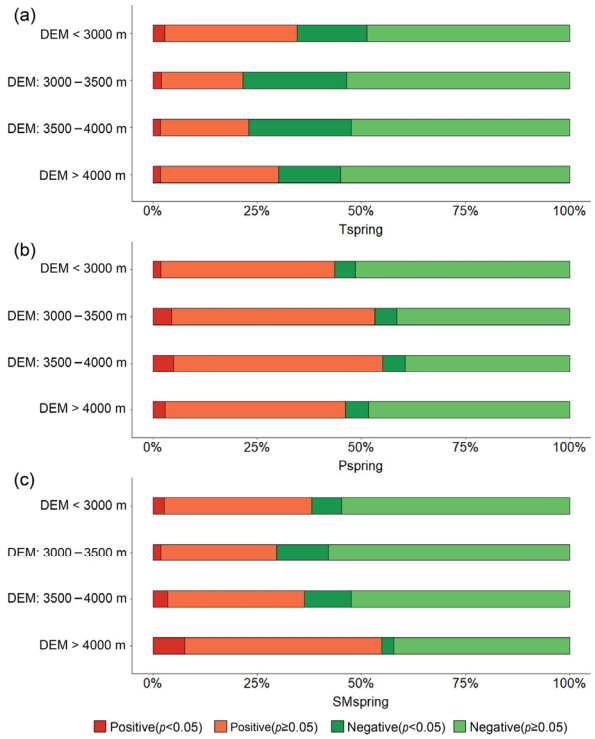

Figure 6. Percentages of correlation between SOS and three driving factors at different elevation zones. The three driving factors were (**a**) spring temperature (Tspring), (**b**) spring precipitation (Pspring), and (**c**) spring soil moisture (SMspring).

At the lowest elevation zone (<3000 m a.s.l.), the EOS was positively correlated with summer temperatures and precipitation in 62.57% and 72.16% of areas, and 8.03% and 18.1% of the areas showed a significant correlation ($p < 0.05$), respectively (Figure 7b,e). Notably, a negative correlation between EOS and summer soil moisture occurred in 80.96% of vegetation pixels at the lowest elevation zone (<3000 m a.s.l.), which was more than four times larger than the positive correlation (19.04%). Approximately 30.06% of the pixels showed a significantly negative correlation between summer soil moisture and EOS ($p < 0.05$) at the lowest elevation zone (<3000 m a.s.l.), while areas with significant positive correlations represented only 0.59% of the total (Figure 7h), indicating that the EOS was advanced in most low elevation regions with an increase in summer soil moisture. A positive correlation between the EOS and autumn temperature covered more than 60% of the area in the different elevation zones, and more than 7.00% of the pixels exhibited a significant correlation (Figure 7c). For the region with elevations less than 4000 m, more than 8.81% of the areas demonstrated a significantly positive correlation between the EOS and autumn soil moisture (Figure 7i). For the regions with elevations of less than 3500 m, the area with a significant positive correlation between the EOS and autumn soil moisture was greater than the EOS and autumn temperature (Figure 7c,i), so at lower elevations (less than 3500 m), soil moisture played a more important role in vegetation growth in autumn. At higher elevations (higher than 3500 m), temperature played a more important role in vegetation growth in autumn (Figure 7c). Overall, compared with autumn temperature and soil moisture, autumn precipitation had a weaker influence on the EOS at the four elevation zones (Figure 7f).

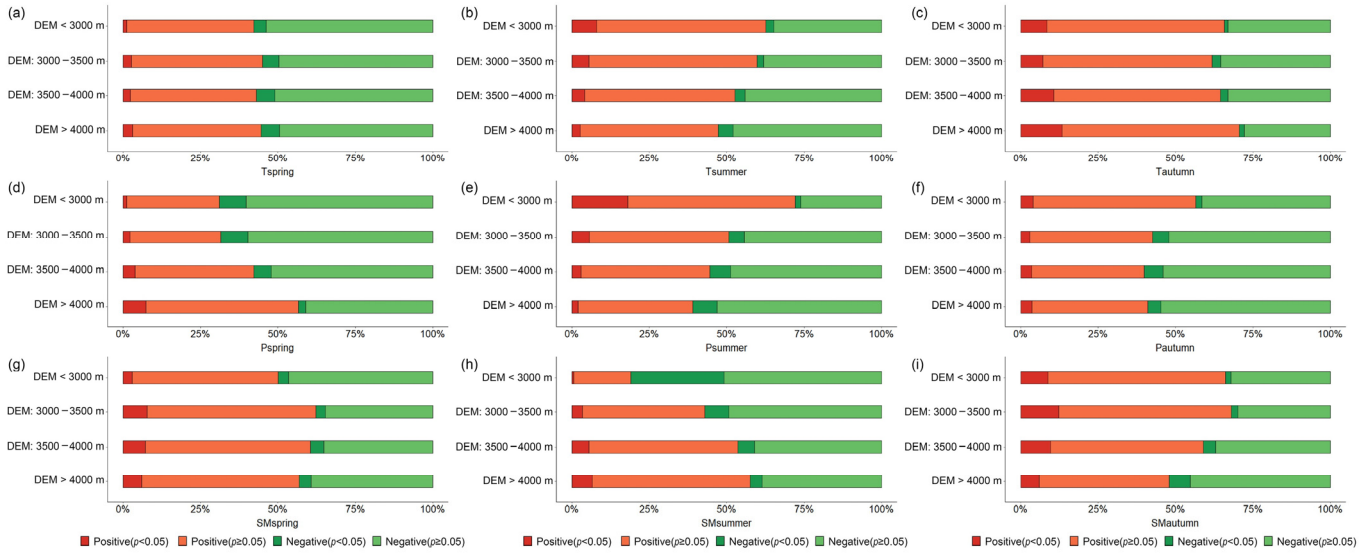

Figure 7. Percentages of correlation between EOS and different driving factors at different elevation zones. The driving factors were (**a**,**b**,**c**) seasonal temperature (Tspring, Tsummer, and Tautumn are spring, summer, and autumn temperature, respectively), (**d**,**e**,**f**) seasonal precipitation (Pspring, Psummer, and Pautumn are spring, summer, and autumn precipitation, respectively), and (**g**,**h**,**i**) seasonal soil moisture (SMspring, SMsummer, and SMautumn are spring, summer, and autumn soil moisture, respectively).

3.4. Vegetation Phenology Response to Seasonal Driving Factors across Vegetation Types

Generally, different vegetation types had different responses to driving factors (Figures 8 and 9). For different vegetation types, the partial correlation coefficients between the SOS and spring temperature were mostly negative (Figure 8a), especially for broadleaf forests, needleleaf forests, shrubland, and meadows (more than 23% of regions had significantly negative correlations). The partial correlation coefficients between the SOS and spring soil moisture were also mostly negative (Figure 8c) for different vegetation types, except alpine vegetation, and more than 7.80% of areas had significantly negative correlations. For alpine vegetation, the SOS was negatively correlated with spring temperature in approximately 65.18% of areas, of which 12.14% of areas showed a significant negative correlation (Figure 8a). However, it was positively correlated with the spring soil moisture in 52.04% of areas, with 7.49% of regions showing a significantly positive correlation (Figure 8c). Compared with spring temperature and soil moisture, spring precipitation had a weaker influence on the SOS in most vegetation types. The areas of positive and negative correlation between spring precipitation and the SOS were similar, with few pixels showing a significant correlation (Figure 8b).

Compared with the correlation between the EOS and autumn temperature and soil moisture, there were limited positive and negative correlations between the EOS and autumn precipitation, and there were relatively few significant pixels for most vegetation types (Figure 9f). Autumn temperature and soil moisture had mainly positive correlations with the EOS for most vegetation types (Figure 9c,i), and the EOS had a more significant relation with soil moisture than temperature for grasslands and deserts. There was a negative correlation between EOS and spring temperature in more than 65% of areas of broadleaf forests, and 13.49% of the areas were significantly correlated (Figure 9a). For needleleaf forests, there was a negative correlation between EOS and spring precipitation in 66.11% of areas, and 10.64% of the areas were significantly correlated (Figure 9d). A significant positive correlation between the EOS and summer precipitation was found in 11.51% of pixels for broadleaf forest and 11.36% of pixels for needleleaf forest (Figure 9e). Summer and autumn soil moisture had opposite correlations with the EOS in QLMs, except meadows. The EOS was mainly negatively correlated with summer soil moisture, especially

for broadleaf forests, needleleaf forests, and grasslands (approximately 15.58%, 14.71%, and 18.78% of the pixels had significant negative correlations, respectively). The EOS of most vegetation types were positively correlated with autumn soil moisture, especially those of grasslands and deserts (for which approximately 11.35% and 12.97% of the pixels had significant positive correlations, respectively).

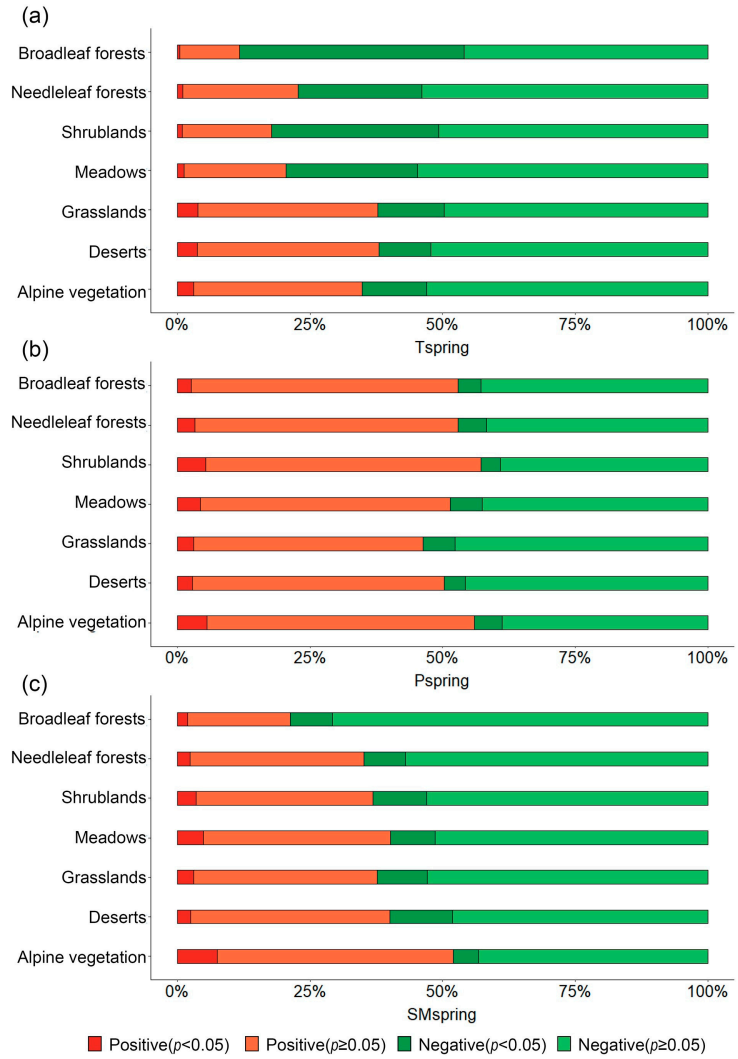

Figure 8. PerPercentages of correlation between the SOS and three driving factors in different vegetation types. The three driving factors were (**a**) spring temperature (Tspring), (**b**) spring precipitation (Pspring), and (**c**) spring soil moisture (SMspring).

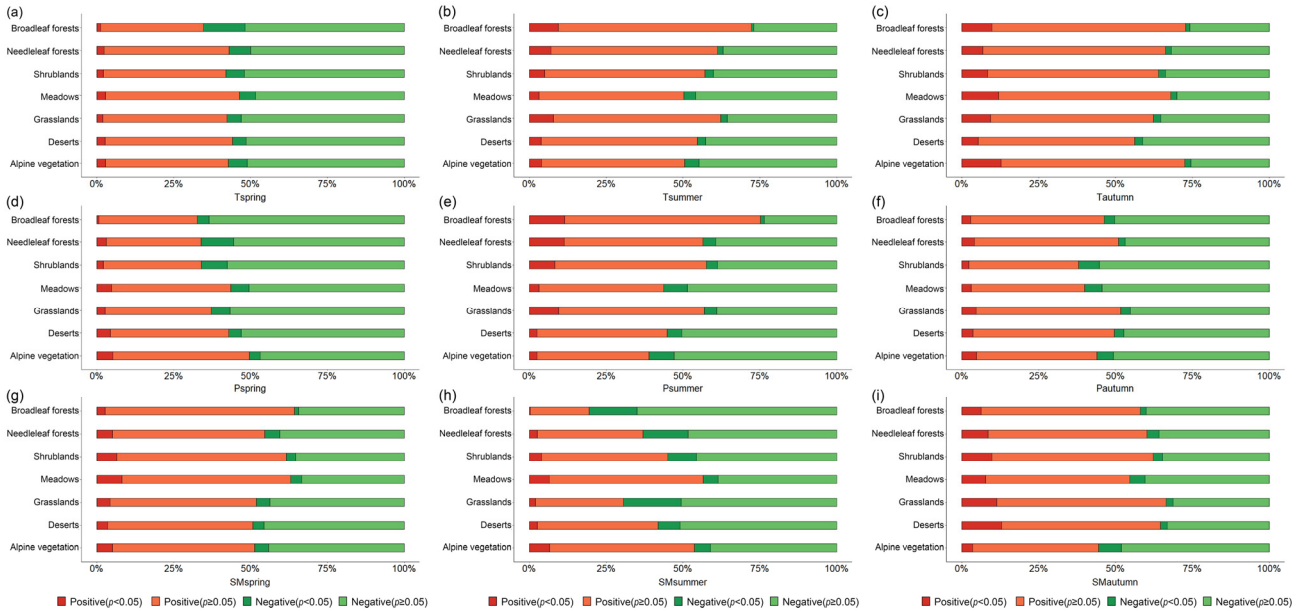

Figure 9. Percentages of correlation between EOS and different driving factors in different vegetation types. The driving factors were (**a**,**b**,**c**) seasonal temperature (Tspring, Tsummer, and Tautumn are spring, summer, and autumn temperature, respectively), (**d**,**e**,**f**) seasonal precipitation (Pspring, Psummer, and Pautumn are spring, summer, and autumn precipitation, respectively), and (**g**,**h**,**i**) seasonal soil moisture (SMspring, SMsummer, and SMautumn are spring, summer, and autumn soil moisture, respectively).

4. Discussion

4.1. The Spatial Heterogeneity of Vegetation Phenology in the Qilian Mountains

The vegetation phenology in the QLMs showed significant spatial heterogeneity. In general, the SOS was later in the central region and earlier in the eastern and western regions of the QLMs, and the EOS exhibited the opposite trend in terms of its spatial distribution. These results are consistent with the results reported by Qi et al. [27] and Sun et al. [35] but inconsistent with the results reported by Qiao et al. [36], who observed that the multiyear mean SOS was gradually delayed from southeast to northwest and that the multiyear mean EOS gradually advanced from southeast to northwest in the QLMs. The main reasons for the differences in the results are the different temporal and spatial resolutions of the remote sensing data. Different remote sensing data sources and data time series may obtain different vegetation phenology results [37,38]. The AVHRR and MODIS datasets have a consistently high temporal resolution time series of data and are widely used for phenology studies [39]. MODIS data (1 km) have a higher resolution than AVHRR data (8 km) and can extract more detailed spatial phenological signals for vegetation types, particularly in heterogeneous areas [40]. The vegetation phenology of the QLMs was characterized by an advanced SOS, delayed EOS, and extended LOS during the period from 2001 to 2020, which are consistent with recent results on the QTP [37,38,41] and on the QLMs [27,35].

In our study, the results showed that the SOS gradually delayed, the EOS gradually advanced, and the LOS gradually shortened with increasing altitude. No significant correlation was found between the SOS and altitude, but a significant negative correlation was found between both the EOS and LOS and altitude. These results are consistent with recent findings on the QTP [2]. The SOS change may have almost nothing to do with altitude [2]. At higher altitudes, there is relatively low air temperature, which is not beneficial for delaying leaf senescence, and the EOS advances to avoid harm from frost and has a shorter LOS [42].

4.2. Response of Vegetation Phenology to Different Driving Factors

Vegetation phenology responses to different driving factors are complex and variable. In our study, we found that the SOS was negatively correlated with spring temperature and spring soil moisture in most regions of the study area, implying that the advanced SOS could be associated with a warmer spring air temperature and higher soil moisture. In our study, the spring temperature had a stronger influence on the SOS, and most studies have also reported that higher temperatures were the main factor associated with an earlier SOS around the world over the last several decades [18,43–45].

The impacts of driving factors on vegetation phenology were varied in different elevation zones. For SOS, spring temperature seemed to be the main factor limiting vegetation growth. The QLMs are located in high altitude areas with low temperatures (the annual mean temperature in most areas is below 0 °C); with an increase in altitude, the temperature gradually decreased (Table 2). Vegetation needs a certain amount of cumulative temperature to green up, so the early stages of vegetation growth are more affected by temperature in relatively cold regions [5,46]. The autumn soil moisture was the main limiting factor at lower elevations (<3500 m a.s.l.), and autumn temperature was the main limiting factor at higher elevations (>3500 m a.s.l.). These results are consistent with the research of Peng et al. [47], which demonstrated that soil moisture was the major limiting factor for the radial growth of Qinghai spruce at the lower elevations of the central QLMs and that temperature was the major limiting factor for radial growth of Qinghai spruce at higher elevations. These results also suggest that vegetation management must take elevation differences into account when facing the challenges of climate change. From Table 2, we can see that the annual average soil moisture at lower elevations (0.31 $m^3 \cdot m^{-3}$) was less than that at higher elevations (0.34 $m^3 \cdot m^{-3}$), so this is one possible reason that the autumn soil moisture had a stronger influence on the EOS in lower elevation zones. The EOS showed a significant negative correlation with summer soil moisture in approximately 30.06% of the pixels in the lowest elevation zones (<3000 m a.s.l.). Peng et al. [47] also found that, during the summer at lower elevations, soil moisture is the most important factor limiting xylem cell differentiation based on the Vaganov–Shashkin model.

Table 2. The annual average soil moisture and temperature from 2001 to 2020 in four elevation zones.

	Soil Moisture ($m^3 \cdot m^{-3}$)	**Temperature (°C)**
DEM < 3000 m	0.31	2.19
DEM: 3000–3500 m	0.31	−0.90
DEM: 3500–4000 m	0.34	−4.67
DEM > 4000 m	0.34	−7.27

At the landscape level, the SOS was negatively correlated with spring temperature in most regions with different vegetation types. More specifically, 42.36%, 23.31%, 31.54%, and 24.83% of the areas of broadleaf forests, needleleaf forests, shrublands, and meadows, respectively, showed a significantly negative correlation between SOS and spring temperature (Figure 8a). This is because the broadleaf forests, needleleaf forests, shrublands, and meadows are mainly located in semi-arid regions (more than 78% of these are located in the semi-arid region) where the climate is relatively humid compared with arid regions; however, the temperature is low in the study area, and higher temperature in spring could decrease the damage from frost and promote spring thawing [5]. The spring soil moisture had a stronger influence on the SOS of deserts (Figure 8c). This is because about 90.37% of deserts are located in arid areas with limited soil water conditions (Table 3). The soil water is an indispensable intermediary used to ensure nutrient substance transport, which is likely to be the main reason for the negative correlation between soil moisture and SOS for deserts. Additionally, there are many shallow-rooted plants in deserts, and these shallow-rooted plants are more sensitive to soil moisture changes than other plants [48,49].

A negative correlation was observed between summer soil moisture and EOS, but a positive correlation was observed between autumn soil moisture and EOS for most vegetation types. This negative correlation shifted to a positive correlation from summer to autumn, indicating that the summer and autumn soil moisture had a great influence on the EOS, but the correlation was the opposite in these two seasons. The main reason for this differential response is that the precipitation in QLMs is mainly concentrated in summer [25], and too much moisture prevents vegetation growth because a high soil moisture can limit the absorption of soil nutrients by vegetation [50]. Ren et al. found that the precipitation played a more important role than temperature in the interannual variation of the SOS and EOS in Inner Mongolia [19]. However, compared with temperature and soil moisture, precipitation had a relatively limited impact on the EOS in the QLMs. This is because precipitation may a have lagged effect on vegetation phenology, meaning that soil moisture is a more straightforward driving factor for vegetation phenology than precipitation and has a number of sources in the QLMs, including precipitation, snowmelt, surface runoff, and groundwater.

Table 3. The annual average soil moisture and temperature from 2001 to 2020 for different vegetation types.

	Soil Moisture ($m^3 \cdot m^{-3}$)	**Temperature (°C)**
Broadleaf forests	0.36	1.72
Needleleaf forests	0.34	−1.49
Shrublands	0.35	−2.05
Meadows	0.36	−4.87
Grasslands	0.29	−0.75
Deserts	0.20	−2.49
Alpine vegetation	0.33	−7.16

4.3. Limitations and Future Work

It should be noted that there may be some limitations to our current study. The number of ground observations of vegetation phenology is insufficient, especially in the central and western parts of the QLMs because of a lack of phenological observation networks. At the same time, the existing observation stations have a relatively short historical record. Digital cameras have been shown to be valuable tools to validate the phenology derived from satellite imagery at a low cost [40] because of their high temporal and spatial resolutions. In future, automated digital cameras are promising for providing consistent and continuous monitoring of vegetation growth at local and regional scales [51,52].

The vegetation phenology results calculated from remote sensing data may contain some uncertainties that are due to the inaccuracy of satellite data. NDVI data have been widely used for phenology characterization because they are simple to measure for most optical sensors [53,54]. However, because NDVI data are sensitive to the soil background and are easily saturated in high vegetation coverage areas [55], the applications of NDVI data may have some limitations. Considering the sparse vegetation in the western part of the QLMs, the modified vegetation index, such as the soil-adjusted vegetation index (SAVI), may be appropriate for detecting vegetation growth changes because of its ability to minimize the effects of the soil background. In the future, collective analyses of multiple VIs (such as the land phenology index, enhanced vegetation index, and perpendicular vegetation index) may improve the accuracy of phenology estimation [56–58]. The spatial resolution of ERA5-Land soil moisture data is relatively low, which may hide some spatial details of soil moisture parameters. But the high-resolution soil datasets are difficult to obtain for a large study area [59]. Future studies should integrate a series of soil moisture datasets at a higher resolution to further discuss the response relationship between vegetation phenology and soil moisture. Vegetation phenology is also influenced by other factors,

such as radiation, soil nutrients, climate extremes, and human activities, so more attention should be paid to exploring the phenology variations in response to these driving factors in future work. The vegetation phenology response to driving factors may be nonlinear, and the interactions between climatic factors have critical role in vegetation phenology, so other methods like the GeoDetector model can be used to detect the contribution of driving factors to vegetation phenology and the interactions between driving factors. Our findings suggest that the variation in soil moisture should be considered in future studies on climate warming and the environmental effects of phenology in water-limited areas.

5. Conclusions

Based on the time series MODIS NDVI datasets from 2001 to 2020, we retrieved the vegetation phenological parameters in the QLMs. The spatiotemporal variation in vegetation phenology was analyzed, and divergent correlations between the SOS and EOS and seasonal driving factors were explored. The results demonstrated that vegetation phenology in the QLMs is characteristic of advancing SOS, postponing EOS, and prolonging LOS, but the variation trends of vegetation phenology were not significant ($p > 0.05$) from 2001 to 2020. The seasonal temperature, precipitation, and soil moisture had spatiotemporal heterogeneous effects on the vegetation phenology. Compared with temperature and soil moisture, precipitation had a weaker influence on the vegetation phenology in QLMs. The spring temperature was the key driving factor influencing SOS in the QLMs. The autumn soil moisture and autumn temperature made the largest contributions to the variations in EOS at lower elevations (<3500 m a.s.l.) and higher elevations (>3500 m a.s.l.), respectively. Spring temperature was the key driving factor influencing SOS of most vegetation types. Autumn soil moisture was the main factor influencing EOS in deserts because of the strong soil moisture stress. An increase in summer soil moisture may limit vegetation growth in the QLMs. Under ongoing global change, finding the response of the SOS and EOS to driving factors is beneficial for a better understanding of the interactions between vegetation phenology and future climate change.

Supplementary Materials: The following supporting information can be downloaded at https://www.mdpi.com/article/10.3390/rs14153645/s1: Figure S1: Comparison of satellite-derived phenology data with ground-based phenology data.

Author Contributions: Formal analysis, X.C.; Methodology, X.C.; Software, G.X. and D.L.; Visualization, G.X. and X.H.; Writing—original draft, X.C.; Writing—review & editing, X.C. All authors have read and agreed to the published version of the manuscript.

Funding: This research was supported by the Strategic Priority Research Program of Chinese Academy of Sciences (grant XDA20100102) and Gansu Provincial Science and Technology Major Special Plan (20ZD7FA005).

Conflicts of Interest: The authors declare no conflict of interest.

References

1. Pau, S.; Wolkovich, E.M.; Cook, B.I.; Davies, T.J.; Kraft, N.J.B.; Bolmgren, K.; Betancourt, J.L.; Cleland, E.E. Predicting phenology by integrating ecology, evolution and climate science. *Glob. Change Biol.* **2011**, *17*, 3633–3643. [CrossRef]
2. Liu, X.; Chen, Y.; Li, Z.; Li, Y.; Zhang, Q.; Zan, M. Driving Forces of the Changes in Vegetation Phenology in the Qinghai–Tibet Plateau. *Remote Sens.* **2021**, *13*, 4952. [CrossRef]
3. Parmesan, C. Ecological and evolutionary responses to recent climate change. *Annu. Rev. Ecol. Evol. Syst.* **2006**, *37*, 637–669. [CrossRef]
4. Peñuelas, J.; Rutishauser, T.; Filella, I. Phenology feedbacks on climate change. *Science* **2009**, *324*, 887–888. [CrossRef]
5. Piao, S.L.; Tan, J.G.; Chen, A.P.; Fu, Y.H.; Ciais, P.; Liu, Q.; Janssens, I.A.; Vicca, S.; Zeng, Z.Z.; Jeong, S.J.; et al. Leaf onset in the northern hemisphere triggered by daytime temperature. *Nat. Commun.* **2015**, *6*, 6911. [CrossRef]
6. Richardson, A.D.; Keenan, T.F.; Migliavacca, M.; Ryu, Y.; Sonnentag, O.; Toomey, M. Climate change, phenology, and phenological control of vegetation feedbacks to the climate system. *Agric. For. Meteorol.* **2013**, *169*, 156–173. [CrossRef]
7. Morisette, J.T.; Richardson, A.D.; Knapp, A.K.; Fisher, J.I.; Graham, E.A.; Abatzoglou, J.; Wilson, B.E.; Breshears, D.D.; Henebry, G.M.; Hanes, J.M.; et al. Tracking the rhythm of the seasons in the face of global change: Phenological research in the 21st century. *Front. Ecol. Environ.* **2009**, *7*, 253–260. [CrossRef]

8. Jin, Z.; Zhuang, Q.; He, J.S.; Luo, T.; Shi, Y. Phenology shift from 1989 to 2008 on the Tibetan Plateau: An analysis with a process-based soil physical model and remote sensing data. *Clim. Change* **2013**, *119*, 435–449. [CrossRef]
9. Xu, Q.; Yang, G.; Long, H.; Wang, C.; Li, X.; Huang, D. Crop information identification based on MODIS NDVI time-series data. *Trans. Chin. Soc. Agric. Eng.* **2014**, *30*, 134–144.
10. Fu, Y.; Zhang, H.C.; Dong, W.J.; Yuan, W.P. Comparison of phenology models for predicting the onset of growing season over the Northern Hemisphere. *PLoS ONE* **2014**, *9*, e109544. [CrossRef]
11. Zhao, X.; Zhou, D.; Fang, J. Satellite-based Studies on Large-Scale Vegetation Changes in China. *J. Integr. Plant Biol.* **2012**, *54*, 713–728. [CrossRef]
12. Fitchett, J.M.; Grab, S.W.; Thompson, D.I. Plant phenology and climate change: Progress in methodological approaches and application. *Prog. Phys. Geogr.* **2015**, *39*, 460–482. [CrossRef]
13. Zhang, F.; Wu, B.; Liu, C.; Luo, Z.; Zhang, S.; Zhang, G. A method to extract regional crop growth profile with time series of NDVI data. *Remote Sens.* **2004**, *8*, 515–528.
14. Wolfe, D.W.; Schwartz, M.D.; Lakso, A.N.; Otsuki, Y.; Pool, R.M.; Shaulis, N.J. Climate Change and Shifts in Spring Phenology of Three Horticultural Woody Perennials in Northeastern USA. *Int. J. Biometeorol.* **2005**, *49*, 303–309. [CrossRef]
15. He, Z.B.; Du, J.; Zhao, W.Z.; Yang, J.J.; Chen, L.F.; Zhu, X.; Chang, X.X.; Liu, H. Assessing temperature sensitivity of subalpine shrub phenology in semi-arid mountain regions of China. *Agric. For. Meteorol.* **2015**, *213*, 42–52. [CrossRef]
16. Menzel, A.; Sparks, T.H.; Estrella, N.; Koch, E.; Aasa, A.; Ahas, R.; Alm-Kübler, K.; Bissolli, P.; Braslavska, O.; Briede, A.; et al. European Phenological Response to Climate Change Matches the Warming Pattern. *Glob. Change Biol.* **2006**, *12*, 1969–1976. [CrossRef]
17. Ge, Q.S.; Wang, H.J.; Rutishauser, T.; Dai, J.H. Phenological Response to Climate Change in China: A Meta-Analysis. *Glob. Change Biol.* **2015**, *21*, 265–274. [CrossRef]
18. Liu, Q.; Fu, Y.H.; Zeng, Z.; Huang, M.T.; Li, X.R.; Piao, S.L. Temperature, precipitation, and insolation effects on autumn vegetation phenology in temperate China. *Glob. Change Biol.* **2016**, *22*, 644–655. [CrossRef]
19. Ren, S.L.; Chen, X.Q.; An, S. Assessing plant senescence reflectance index-retrieved vegetation phenology and its spatiotemporal response to climate change in the Inner Mongolian Grassland. *Int. J. Biometeorol.* **2017**, *61*, 601–612. [CrossRef]
20. Luo, M.; Meng, F.H.; Sa, C.L.; Duan, Y.C.; Bao, Y.H.; Liu, T.; De Maeyer, P. Response of vegetation phenology to soil moisture dynamics in the Mongolian Plateau. *CATENA* **2021**, *206*, 105505. [CrossRef]
21. Cleverly, J.; Eamus, D.; Coupe, N.R.; Chen, C.; Maes, W.; Li, L.; Faux, R.; Santini, N.S.; Rumman, R.; Yu, Q.; et al. Soil moisture controls on phenology and productivity in a semi-arid critical zone. *Sci. Total Environ.* **2016**, *568*, 1227–1237. [CrossRef]
22. Garonna, I.; De Jong, R.; De Wit, A.J.W.; Mucher, C.A.; Schmid, B.; Schaepman, M.E. Strong contribution of autumn phenology to changes in satellite-derived growing season length estimates across Europe (1982–2011). *Glob. Change Biol.* **2014**, *20*, 3457–3470. [CrossRef]
23. Song, L.L.; Tian, Q.; Li, Z.J.; Lv, Y.M.; Gui, J.; Zhang, B.J.; Cui, Q. Changes in characteristics of climate extremes from 1961 to 2017 in Qilian Mountain area, northwestern China. *Environ. Earth Sci.* **2022**, *81*, 177. [CrossRef]
24. Lin, P.F.; He, Z.B.; Du, J.; Chen, L.F.; Zhu, X.; Li, J. Recent changes in daily climate extremes in an arid mountain region, a case study in northwestern China's Qilian Mountains. *Sci. Rep.* **2017**, *7*, 2245. [CrossRef]
25. Gou, X.H.; Zhang, F.; Deng, Y.; Ettl, G.J.; Yang, M.X.; Gao, L.L.; Fang, K.Y. Patterns and dynamics of tree-line response to climate change in the eastern Qilian Mountains, northwestern China. *Dendrochronologia* **2012**, *30*, 121–126. [CrossRef]
26. Sun, F.; Lü, Y.; Wang, J.; Hu, J.; Fu, B. Soil moisture dynamics of typical ecosystems in response to precipitation: A monitoring-based analysis of hydrological service in the Qilian Mountains. *CATENA* **2015**, *129*, 63–75. [CrossRef]
27. Qi, Y.; Wang, H.W.; Ma, X.F.; Zhang, J.L.; Yang, R. Relationship between vegetation phenology and snow cover changes during 2001–2018 in the Qilian Mountains. *Ecol. Indic.* **2021**, *133*, 108351. [CrossRef]
28. Zhang, L.F.; Yan, H.W.; Qiu, L.S.; Cao, S.P.; He, Y.; Pang, G.J. Spatial and Temporal Analyses of Vegetation Changes at Multiple Time Scales in the Qilian Mountains. *Remote Sens.* **2021**, *13*, 5046. [CrossRef]
29. Zhou, L.; Tucker, C.J.; Kaufmann, R.K.; Slayback, D.; Shabanov, N.V.; Myneni, R.B. Variations in northern vegetation activity inferred from satellite data of vegetation index during 1981 to 1999. *J. Geophys. Res. Atmos.* **2001**, *106*, 20069–20083. [CrossRef]
30. Peng, S. 1-km monthly precipitation dataset for China (1901–2020). *Natl. Tibet. Plateau Data Center.* **2020**. [CrossRef]
31. Gonsamo, A.; Chen, J.M.; Ooi, Y.W. Peak season plant activity shift towards spring is reflected by increasing carbon uptake by extratropical ecosystems. *Glob. Change Biol.* **2018**, *24*, 2117–2128. [CrossRef] [PubMed]
32. Akritas, M.G.; Murphy, S.A.; Lavalley, M.P. The Theil-Sen estimator with doubly censored data and applications to astronomy. *Am. Stat. Assoc.* **1995**, *90*, 170–177. [CrossRef]
33. Wang, X.Y.; Wu, C.Y. Estimating the peak of growing season (POS) of China's terrestrial ecosystems. *Agric. For. Meteorol.* **2019**, *278*, 107639. [CrossRef]
34. Hamed, K.H. Trend detection in hydrologic data: The Mann–Kendall trend test under the scaling hypothesis. *J. Hydrol.* **2008**, *349*, 350–363. [CrossRef]
35. Sun, Y.F.; Guan, Q.Y.; Wang, Q.Z.; Yang, L.Q.; Pan, N.H.; Ma, Y.R.; Luo, H.P. Quantitative assessment of the impact of climatic factors on phenological changes in the Qilian Mountains, China. *For. Ecol. Manag.* **2021**, *499*, 119594. [CrossRef]
36. Qiao, C.; Shen, S.; Cheng, C.; Wu, J.; Jia, D.; Song, C. Vegetation Phenology in the Qilian Mountains and Its Response to Temperature from 1982 to 2014. *Remote Sens.* **2021**, *13*, 286. [CrossRef]

37. Piao, S.; Cui, M.; Chen, A.; Wang, X.; Ciais, P.; Liu, J.; Tang, Y. Altitude and temperature dependence of change in the spring vegetation green-up date from 1982 to 2006 in the Qinghai-Xizang Plateau. *Agric. For. Meteorol.* **2011**, *151*, 1599–1608. [CrossRef]
38. Shen, M.G.; Piao, S.L.; Dorji, T.; Liu, Q.; Cong, N.; Chen, X.Q.; An, S.; Wang, S.P.; Wang, T.; Zhang, G.X. Plant phenological responses to climate change on the Tibetan Plateau: Research status and challenges. *Natl. Sci. Rev.* **2015**, *2*, 454–467. [CrossRef]
39. Zeng, L.L.; Wardlow, B.D.; Xiang, D.X.; Hu, S.; Li, D.R. A review of vegetation phenological metrics extraction using time-series, multispectral satellite data. *Remote Sens. Environ.* **2020**, *237*, 111511. [CrossRef]
40. Tao, Z.X.; Huang, W.J.; Wang, H.J. Soil moisture outweighs temperature for triggering the green-up date in temperate grasslands. *Theor. Appl. Climatol.* **2020**, *140*, 1093–1105. [CrossRef]
41. Huang, K.; Zu, J.X.; Zhang, Y.J.; Cong, N.; Liu, Y.J.; Chen, N. Impacts of snow cover duration on vegetation spring phenology over the Tibetan Plateau. *J. Plant Ecol.* **2018**, *12*, 583–592. [CrossRef]
42. Chen, L.; Hänninen, H.; Rossi, S.; Smith, N.G.; Pau, S.; Liu, Z.; Feng, G.; Gao, J.; Liu, J. Leaf senescence exhibits stronger climatic responses during warm than during cold autumns. *Nat. Clim. Change* **2020**, *10*, 777–780. [CrossRef]
43. Cleland, E.E.; Chuine, I.; Menzel, A.; Mooney, H.A.; Schwartz, M.D. Shifting plant phenology in response to global change. *Trends. Ecol. Evol.* **2007**, *22*, 357–365. [CrossRef]
44. Che, M.L.; Chen, B.Z.; Innes, J.L.; Wang, G.Y.; Dou, X.M.; Zhou, T.M.; Zhang, H.F.; Yan, J.W.; Xu, G.; Zhao, H.W. Spatial and temporal variations in the end date of the vegetation growing season throughout the Qinghai-Tibetan Plateau from 1982 to 2011. *Agric. For. Meteorol.* **2014**, *189*, 81–90. [CrossRef]
45. Yang, Y.T.; Guan, H.D.; Shen, M.G.; Liang, W.; Jiang, L. Changes in autumn vegetation dormancy onset date and the climate controls across temperate ecosystems in China from 1982 to 2010. *Glob. Change Biol.* **2015**, *21*, 652–665. [CrossRef]
46. Shen, M.G.; Tang, Y.H.; Chen, J.; Zhu, X.L.; Zheng, Y.H. Influences of temperature and precipitation before the growing season on spring phenology in grasslands of the central and eastern Qinghai-Tibetan Plateau. *Agric. For. Meteorol.* **2011**, *151*, 1711–1722. [CrossRef]
47. Peng, X.M.; Du, J.; Yang, B.; Xiao, S.C.; Li, G. Elevation-influenced variation in canopy and stem phenology of Qinghai spruce, central Qilian Mountains, northeastern Tibetan Plateau. *Trees* **2019**, *33*, 707–717. [CrossRef]
48. Derner, J.D.; Hess, B.W.; Olson, R.A.; Schuman, G.E. Functional group and species responses to precipitation in three semi-arid rangeland ecosystems. *Arid Land Res. Manag.* **2008**, *22*, 81–92. [CrossRef]
49. Dorji, T.; Totland, O.; Moe, S.R.; Hopping, K.A.; Pan, J.B.; Klein, J.A. Plant functional traits mediate reproductive phenology and success in response to experimental warming and snow addition in Tibet. *Glob. Chang. Biol.* **2013**, *19*, 459–472. [CrossRef]
50. Zhang, R.R.; Qi, J.Y.; Leng, S.; Wang, Q.F. Long-term vegetation phenology changes and responses to preseason temperature and precipitation in Northern China. *Remote Sens.* **2022**, *14*, 1396. [CrossRef]
51. Zhang, X.Y.; Jayavelu, S.; Liu, L.L.; Friedl, M.A.; Henebry, G.M.; Liu, Y.; Schaaf, C.B.; Richardson, A.D.; Gray, J. Evaluation of land surface phenology from VIIRS data using time series of PhenoCam imagery. *Agric. For. Meteorol.* **2018**, *256*, 137–149. [CrossRef]
52. Sonnentag, O.; Hufkens, K.; Teshera-Sterne, C.; Young, A.M.; Friedl, M.; Braswell, B.H.; Milliman, T.; O'Keefe, J.; Richardson, A.D. Digital repeat photography for phenological research in forest ecosystems. *Agric. For. Meteorol.* **2012**, *152*, 159–177. [CrossRef]
53. Fischer, A. A model for the seasonal variations of vegetation indices in coarse resolution data and its inversion to extract crop parameters. *Remote Sens. Environ.* **1994**, *48*, 220–230. [CrossRef]
54. Moody, A.; Johnson, D.M. Land-surface phenologies from AVHRR using the discrete fourier transform. *Remote Sens. Environ.* **2001**, *75*, 305–323. [CrossRef]
55. Huete, A.; Didan, K.; Miura, T.; Rodriguez, E.P.; Gao, X.; Ferreira, L.G. Overview of the radiometric and biophysical performance of the MODIS vegetation indices. *Remote Sens. Environ.* **2002**, *83*, 195–213. [CrossRef]
56. Walker, J.J.; de Beurs, K.; Wynne, R.H. Dryland vegetation phenology across an elevation gradient in Arizona, USA, investigated with fused MODIS and Landsat data. *Remote Sens. Environ.* **2014**, *144*, 85–97. [CrossRef]
57. Wu, C.Y.; Gonsamo, A.; Gough, C.M.; Chen, J.M.; Xu, S.G. Modeling growing season phenology in North American forests using seasonal mean vegetation indices from MODIS. *Remote Sens. Environ.* **2014**, *147*, 79–88. [CrossRef]
58. Gonsamo, A.; Chen, J.M.; Price, D.T.; Kurz, W.A.; Wu, C.Y. Land surface phenology from optical satellite measurement and CO_2 eddy covariance technique. *J. Geophys. Res. Biogeosci.* **2012**, *117*, 1472. [CrossRef]
59. Kim, J.B.; Kerns, B.K.; Drapek, R.J.; Pitts, G.S.; Halofsky, J.E. Simulating vegetation response to climate change in the Blue Mountains with MC2 dynamic global vegetation model. *Clim. Serv.* **2018**, *10*, 20–32. [CrossRef]